JACS Au
AN OPEN ACCESS JOURNAL OF THE AMERICAN CHEMICAL SOCIETY

pubs.acs.org/jacsau

Article

Two-Dimensional Cationic Aluminoborate as a New Paradigm for Highly Selective and Efficient Cr(VI) Capture from Aqueous Solution

Shuang Wang, Pu Bai, Magdalena Ola Cichocka, Jung Cho, Tom Willhammar, Yunzheng Wang, Wenfu Yan,* Xiaodong Zou,* and Jihong Yu*

Cite This: *JACS Au* 2022, 2, 1669−1678

Read Online

ACCESS | Metrics & More | Article Recommendations | Supporting Information

ABSTRACT: Water pollutants existing in their oxyanion forms have high solubility and environmental mobility. To capture these anionic pollutants, cost-effective inorganic materials with cationic frameworks and outstanding removal performance are ideal adsorbents. Herein, we report that two-dimensional (2D) cationic aluminoborate BAC(10) sets a new paradigm for highly selective and efficient capture of Cr(VI) and other oxyanions from aqueous solution. The structure of Cr(VI)-exchanged BAC(10) sample (Cr(VI)@BAC(10), $H_{0.22}{\cdot}Al_2BO_{4.3}{\cdot}(HCrO_4)_{0.22}{\cdot}2.64H_2O$) has been successfully solved by continuous rotation electron diffraction. The crystallographic data show that the 2D cationic layer of BAC(10) is built by AlO_6 octahedra, BO_4 tetrahedra, and BO_3 triangles. Partial chromate ions exchanged with Cl^- ions are located within the interlayer region, which are chemically bonded to the aluminoborate layer. BAC(10) shows faster adsorption kinetics compared to the commercial anion exchange resin (AER) and layered double hydroxides (LDHs), a higher maximum adsorption capacity of 139.1 mg/g than that of AER (62.77 mg/g), LDHs (81.43 mg/g), and a vast majority of cationic MOFs, and a much broader working pH range (2−10.5) than LDHs. Moreover, BAC(10) also shows excellent Cr(VI) oxyanion removal performance for a solution with a low concentration (1−10 mg/L), and the residual concentration can be reduced to below 0.05 mg/L of the WHO drinking water criterion. These superior properties indicate that BAC(10) is a promising material for remediation of Cr(VI) and other harmful oxyanions from wastewater.

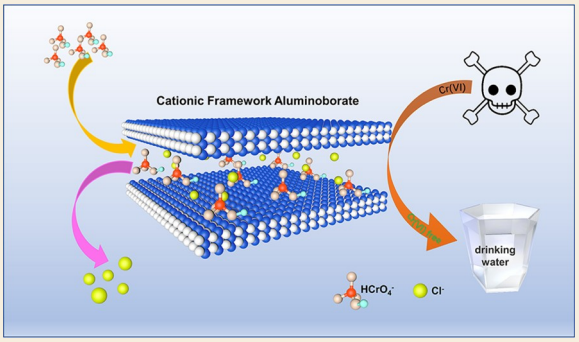

KEYWORDS: *aluminoborate, cationic frameworks, anion exchange, metal oxyanions, selective capture*

INTRODUCTION

Water scarcity and quality degradation due to the contamination of harmful ions have become a worldwide crisis in the 21st century, and thus there is an urgent demand to remove trace contaminants of harmful ions from polluted water. A large number of water-soluble ionic contaminants inherently exist in their oxyanion forms, such as CrO_4^{2-}, TcO_4^-, SeO_4^{2-}, MoO_4^{2-}, VO_4^{3-}, PO_4^{3-}, and AsO_4^{3-}.[1,2] Compared to the cationic pollutants that can be easily removed by adsorption or precipitation,[3] oxyanions have higher solubility and mobility and transfer easily in the environment because the surface of soil or mineral is usually negatively charged due to its low isoelectric point, which makes the oxyanions often poorly sorbed.[4]

Among the harmful oxyanions, Cr(VI) has been identified as one of the 17 chemicals posing the greatest threat to humans and has also been included in the group A of human carcinogens due to its carcinogenicity, mutagenicity, and mobility.[5] According to the regulations of the World Health Organization (WHO), the highest level of total Cr allowed in drinking water is 0.05 mg/L, which has been adopted by European Union and China.[6−8] To meet such a strict criterion, methods for the efficient removal of Cr(VI) from aqueous environmental systems are highly needed.

So far, several methods for removal of Cr(VI) and other oxyanion pollutants from aqueous solution have been reported, including chemical precipitation,[9] adsorption,[10] photocatalytic reduction,[11] and membrane filtration.[12] However, most of these methods have the disadvantages of high costs, complicated operating processes, or low removal efficiencies, especially at low concentrations of Cr(VI). Compared to these methods, anion exchange is considered as a cost-effective, simple, and highly efficient method for removal of oxyanion pollutants at low levels and point-of-use applications.[13−15]

Significant efforts have been made in the past two decades to prepare anion exchangers for removal of oxyanion pollutants.[16−19] Anion exchange resins (AERs) with amino-

Received: April 17, 2022
Revised: June 14, 2022
Accepted: June 16, 2022
Published: June 30, 2022

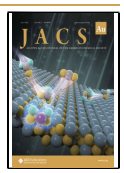

ACS Publications

© 2022 The Authors. Published by American Chemical Society

https://doi.org/10.1021/jacsau.2c00237
JACS Au 2022, 2, 1669−1678

functional groups are the most commonly used anion exchangers and show good performance for oxyanion removal.[20−22] However, they still face many challenges in practical application because of the high cost and limited thermal and chemical stability originating from their organic nature. Recently, cationic metal−organic frameworks (MOFs) have been extensively investigated and outstanding results have been obtained in the fields of oxyanion pollutant removal and catalysis.[23−28] Nevertheless, the commercialization of MOFs is still hampered by their high cost and limited stability in aqueous solution.

To address these shortcomings, a series of cationic inorganic frameworks exhibiting enhanced thermal and hydrolytic stability has been prepared.[29,30] Notably, layered double hydroxides (LDHs) consisting of cationic brucite-type layers charge balanced by interlayer anions have received extensive attention as the next generation of inorganic anion exchangers.[31,32] LDHs have shown excellent removal efficiency for a variety of harmful oxyanions including chromate,[33] phosphate,[34] arsenate,[35] and selenate.[36] However, high-temperature calcination (usually at or above 450 °C) is usually required before their usage, which is a heavy energy consumption process.[37] In addition, other disadvantages for LDHs include the slow adsorption kinetics and poor selectivity, especially in the presence of bicarbonate and carbonate.[38]

In the past decade, a series of hydroxides and fluorides of heavy p-block metals that possess 2D cationic inorganic layers has also been reported.[39−42] The interlayer anions can be exchanged, thus allowing for the removal of oxyanion pollutants from a solution. Nevertheless, the heavy metal nature of such layered materials limits their practical application. Meanwhile, a series of layered rare-earth hydroxides with a 2D cationic inorganic layer has also been synthesized in which $Y_2(OH)_5Cl{\cdot}1.5H_2O$ has been used for removing SeO_4^{2-} and SeO_3^{2-} from aqueous solution.[43,44] However, the use of lanthanides in large doses restricts their practical use. Notre Dame thorium borate-1 (NDTB-1), the first three-dimensional (3D) inorganic cationic extended framework, could selectively remove $^{99}TcO_4^-$ from radioactive waste in the presence of a large excess of competing anions.[45−47] However, the radioactive nature of thorium in the cationic framework of NDTB-1 would seriously limit its further application. Thus, it is highly desirable to seek stable and cost-effective materials with pure inorganic cationic frameworks, high capacities, fast kinetics, and good selectivity toward toxic oxyanions.

Recently, we reported a new type of layered cationic aluminum oxyhydroxide, JU-111, which was hydrothermally synthesized with low-cost raw materials.[48] Such a 2D material exhibits extraordinary performance for Cr(VI) removal even in the presence of a large excess of CO_3^{2-} and has a broad working pH range, which is promising for toxic metal oxyanion remediation.

In our earlier study, we synthesized aluminoborate with a pure inorganic cationic framework, namely BAC(10) ($[H_{0.4}Al_2BO_{4.5}]Cl_{0.4}{\cdot}3H_2O$).[49] The cationic framework of BAC(10) is built up from triangular BO_3, tetrahedral BO_4, and octahedra AlO_6 whose positive charges are balanced by Cl^- anions. The water adsorption of 20 wt % BAC(10) is comparable to that of zeolites, indicating the open-framework nature of BAC(10). Thermogravimetric analysis−mass spectrometry (TGA−MS) and titration analyses confirmed the existence of freely movable Cl^- in the cationic framework of BAC(10), which can be exchanged by Br^-. This indicates that BAC(10) is a promising candidate for Cr(VI) removal. Unfortunately, the structure of BAC(10) is difficult to be solved due to the ultrathin sheet-like morphology of the material.

In this context, we made further investigations on the structure of BAC(10) and its capture ability for Cr(VI) from aqueous solution. The structure of the Cr(VI)@BAC(10) sample could be successfully solved by continuous rotation electron diffraction (cRED), a data collection protocol of 3D electron diffraction including crystal tracking. The adsorption kinetics, isotherm, selectivity, removal efficiency at low concentrations, and reusability of Cr(VI) on BAC(10) were systematically studied using a batch method. In addition, the removal efficiency of other oxyanion pollutants such as ReO_4^-, MoO_4^{2-}, SeO_4^{2-}, $H_2PO_4^-$, and VO_4^{3-} was also investigated. The Cr(VI) oxyanion removal ability of BAC(10) was compared with that of other types of commercial cationic sorbents such as LDHs and AER, which clearly demonstrated its advantages in terms of adsorption capacity and adsorption kinetics. To the best of our knowledge, the 2D cationic framework aluminoborate creates a new paradigm in the removal of harmful oxyanions from water, which may open up new possibilities for its application in many other aspects.

RESULTS AND DISCUSSION

Synthesis and Characterization of BAC(10)

Highly crystalline aluminoborate BAC(10) was hydrothermally synthesized from a mixture of boric acid, anhydrous aluminum trichloride, and ammonium hydroxide at 150 °C for 18 h. The detailed information on synthesis is provided in the Supporting Information.

Figure 1 shows the powder X-ray diffraction (PXRD) patterns of as-synthesized and calcined BAC(10) at 150, 200, 250, and 300 °C for 2 h. As can be seen, the intensity of the characteristic diffraction peaks of BAC(10) decreases with the increase of heating temperature. When the heating temperature reaches 300 °C, the strongest diffraction peak at 10.36° (i.e., (020) according to the later structure solution) almost disappears, indicating that the long-range ordering of

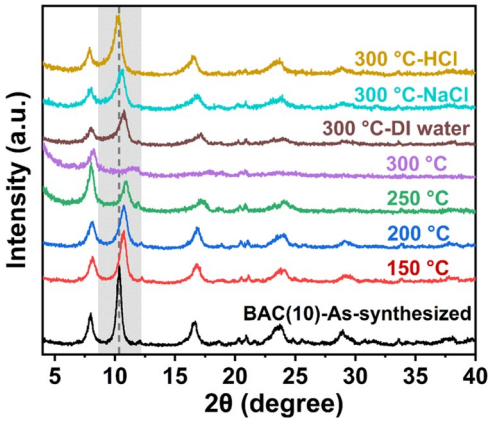

Figure 1. Experimental PXRD patterns of as-synthesized, calcined BAC(10) at 150, 200, 250, and 300 °C for 2 h and the regenerated BAC(10) (immersing calcined BAC(10) in DI water, 0.01 M NaCl, or 0.01 M HCl solution for 24 h).

https://doi.org/10.1021/jacsau.2c00237
JACS Au 2022, 2, 1669−1678

BAC(10) has been almost destroyed at 300 °C. As observed in Figure 1, the positions of most characteristic diffraction peaks of BAC(10) shift to a higher angle during the heating process, suggesting that the aluminoborate structure gradually shrinks during heating. Interestingly, the structure of BAC(10) can be regenerated by immersing the 300 °C calcined BAC(10) in deionized (DI) water, 0.01 M NaCl, or 0.01 M HCl solution, as shown by the PXRD patterns in Figure 1. The recovery process can be described as a "structural memory effect," which has been often observed in LDHs.[26] HCl solution gives the best recovery followed by NaCl solution and DI water. Structure recovery in DI water indicates that the adsorbed H_2O molecules refill the void space after the removal of guest species in BAC(10) by calcination; a better structure recovery in NaCl solution implies that the resorption of Cl^- strengthens the filling effect; the best structure recovery in HCl solution suggests that the acidic environment will further facilitate the repair of the damage in the long-range ordering of BAC(10) due to dehydration at high temperatures.

Scanning electron microscopy (SEM, Figure 2a,b) and low-magnification transmission electron microscopy (TEM, Figure 2c,d) images of the as-synthesized BAC(10) show that the product consists of aggregates of nanosheet-like hexagon-shaped crystals with a length of 3−5 μm and a width of 0.5−1 μm, implying that BAC(10) might have a layered structure or the growth along the direction perpendicular to the sheet is significantly restrained. The corresponding atomic force microscopy (AFM) image (Figure 2e) shows that the average thickness of the nanosheet is about 4.5 nm. The energy-dispersive X-ray spectroscopy (EDS) mapping profile clearly reveals that the as-synthesized BAC(10) contains homogeneously distributed Al, B, O, and Cl elements (Figure 2f−i).

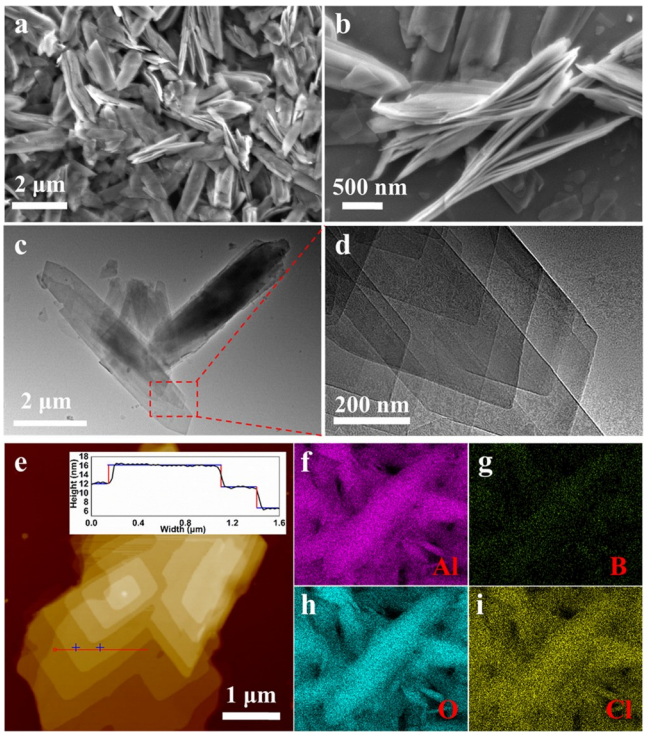

Figure 2. SEM (a,b), TEM (c,d), and AFM (e) images of the as-synthesized BAC(10); EDS mapping profiles of BAC(10) for Al (f), B (g), O (h), and Cl (i).

Physicochemical Properties and Structural Analysis of Cr(VI)@BAC(10)

Anion exchange experiments were conducted at 25 °C using a batch sorption method, and the detailed information is provided in the Supporting Information. Figure 3a shows the PXRD patterns of BAC(10) before and after adsorption of Cr(VI), which is denoted as Cr(VI)@BAC(10). PXRD data reveal that the main structure of BAC(10) is retained after the adsorption of Cr(VI). However, the crystallinity is obviously decreased. A TEM analysis on Cr(VI)@BAC(10) (Figure S1) reveals that the lamellar morphology of BAC(10) is maintained after Cr(VI) adsorption. The EDS mapping profiles of BAC(10) and Cr(VI)@BAC(10) also confirm that the adsorption of Cr(VI) from aqueous solution follows an anion exchange process of Cl^- existing in the framework of BAC(10) (Figure S2). The Fourier transform infrared (FTIR) spectrum of Cr(VI)@BAC(10) shows an adsorption peak at 921 cm^{-1} that is not present in the spectrum of BAC(10) (Figure 3b). This peak can be assigned to the antisymmetric $Cr^{VI}O_3$ stretching vibration, confirming the incorporation of Cr(VI) anions inside the structure of BAC(10).[50] Figure 3c shows the X-ray photoelectron spectroscopy (XPS) spectra of BAC(10) and Cr(VI)@BAC(10). In Figure 3c, the peak from element Cl (198.5 eV, Cl 2p) is clearly observed in the spectrum of BAC(10). After Cr(VI) adsorption, the Cl 2p peak at 198.5 eV completely disappears and a new Cr 2p peak at about 580 eV appears simultaneously. Figure 3d shows the high-resolution XPS spectra of the Cr 2p region. Compared to K_2CrO_4, the Cr 2p peaks of Cr(VI)@BAC(10) are slightly blueshifted. The spectra of Cr(VI)@BAC(10) have two main peaks, that is, Cr $2p_{1/2}$ (589.5 eV) and Cr $2p_{3/2}$ (579.7 eV), which correspond to Cr(VI). The minor signals with binding energies of 586.5 and 576.9 eV are attributed to the trace amount of Cr(III) formed from the known reduction effects under X-ray irradiation.[51] The TGA results show that the total weight loss of BAC(10) and Cr(VI)@BAC(10) between 100 and 800 °C is 33.3 and 26.1%, respectively (Figure 3e). The TGA−MS analysis on BAC(10) and Cr(VI)@BAC(10) (Figure 3f) shows that HCl is released from BAC(10) at above 250 °C, and no detectable HCl is released from Cr(VI)@BAC(10) at the entire temperature range. The nitrogen adsorption analysis gives a BET surface area of 35.6 m^2/g for Cr(VI)@BAC(10), which is smaller than that of 59.3 m^2/g for as-synthesized BAC(10) (Figure S3), which is consistent with the decrease in crystallinity after the adsorption of Cr(VI) (Figure 3a). Combining the above characterization results, it can be concluded that: (1) the Cl^- ions in the structure of BAC(10) are exchangeable; (2) Cr(VI) anions are incorporated inside the framework of BAC(10) via anion exchange; and (3) all Cl^- ions can be exchanged by Cr(VI) anions under such conditions.

For inspection of the Cr(VI)@BAC(10) crystalline structure, cRED data were collected using a TEM (Figure S4). The 3D reciprocal lattice reconstructed from the cRED data using the software RED[52] shows that Cr(VI)@BAC(10) is monoclinic with the unit cell parameters a = 16.020(3) Å, b = 16.910(3) Å, c = 16.390(3) Å, and β = 112.69(3)° (Figure 4). Because the nanosheets, which are perpendicular to the b-axis, have only a few unit cells, weak diffuse streaks along the b^*-axis were observed for most reflections (Figure S5). Despite this, the intensities of reflections could be extracted from the cRED data. The aluminoborate structure Cr(VI)@BAC(10) was solved by direct methods using the space group $P21/n$

https://doi.org/10.1021/jacsau.2c00237
JACS Au 2022, 2, 1669−1678

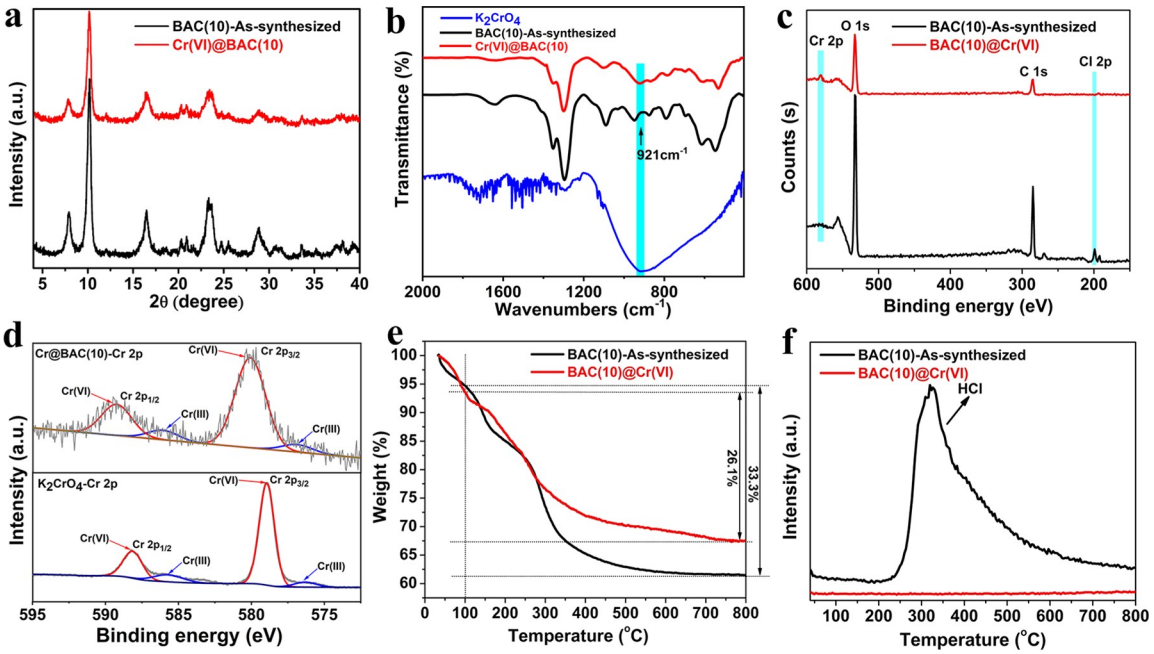

Figure 3. PXRD (a), FTIR (b), and XPS (c) results of BAC(10) and Cr(VI)@BAC(10); (d) high-resolution Cr $2p_{1/2}$ and Cr $2p_{3/2}$ core-level XPS spectra of Cr(VI)@BAC(10) and K_2CrO_4; TGA (e) and TGA–MS (f) of BAC(10) and Cr(VI)@BAC(10).

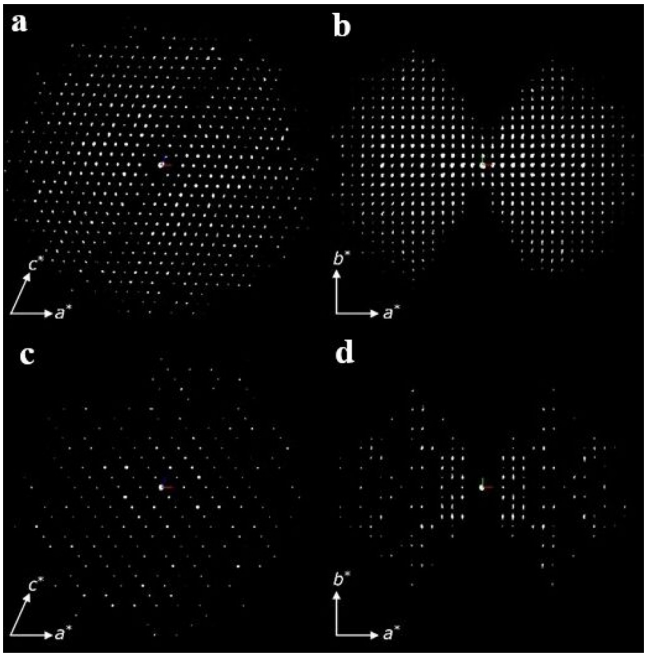

Figure 4. (a,b) 3D reciprocal lattice of Cr(VI)@BAC(10) viewed along *b**- and *c**-axes, respectively. Only strong reflections are shown. (c,d) 2D slices of *h*0*l* and *hk*0 of the 3D reciprocal lattice in panel (b), respectively. The systematic absence could be deduced as *hkl*, 0*kl*, *hk*0: none, *h*0*l*: $h + l = 2n$, and that along 0*k*0 could not be determined due to the preferred orientation around the *b**-axis. The possible space groups are then *Pn* (No. 7), *P*2/*n* (No. 13), and $P2_1/n$ (No. 14).

(No. 14), which is very complex with 62 (12 aluminum, 6 boron, and 44 oxygen) atoms in the asymmetric unit. Three chromate ions were located from the difference Fourier maps, which were subsequently refined to an occupancy of 0.77 (CrA), 0.32 (CrB), and 0.24 (CrC). The refinement against the cRED data converged to $R1 = 0.2769$ for 2771 reflections with $I > 2I(\sigma)$ and $R1 = 0.2983$ for all 3541 reflections [CCDC-2127099]. More details of structure determination are described in the Supporting Information (Section 7, Table S1, and Figures S6,S7).

The framework of Cr(VI)@BAC(10) ($H_{0.22}{\cdot}Al_2BO_{4.3}{\cdot}(HCrO_4)_{0.22}{\cdot}2.64H_2O$) has a cationic layered structure, built by AlO_6 octahedra, BO_4 tetrahedra, and BO_3 triangles. The AlO_6 octahedra are linked by edge- or corner-sharing to form a layer with exclusively six rings (Figure 5a). The six rings are decorated by either BO_3 or BO_4. Three-coordinated boron atoms are found in the six rings with only one or two corner-sharing AlO_6 octahedra; each boron is coordinated to three edge-sharing oxygen atoms. Tetrahedrally coordinated boron atoms are located in the six rings with three corner-sharing

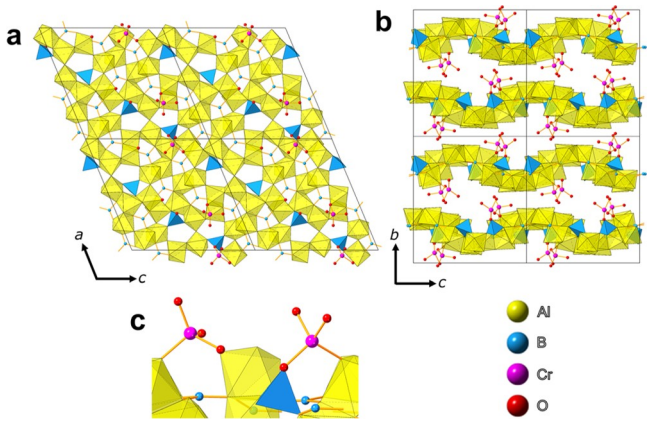

Figure 5. Structure of Cr(VI)@BAC(10) viewed along (a) [010] and (b) [100] directions. Only one layer is shown in panel (a). A total of four CrO_4^- binding sites are shown, of which two are partially occupied (77 and 32%, respectively). The empty sites are marked by bare oxygen atoms. (c) Connections of two chromates CrA and CrB to the aluminoborate layer. The third chromate (CrC) is not shown for clarity.

https://doi.org/10.1021/jacsau.2c00237
JACS Au 2022, 2, 1669–1678

AlO_6 octahedral pairs; each BO_4 is connected to one edge-sharing and two terminal oxygens in the AlO_6 octahedral layer, with one terminal oxygen pointing away from the layer (Figure 5a). There are two layers in each unit cell, and the layers are sinusoidal along the *c*-axis (Figure 5b). Adjacent layers are held together by hydrogen bonding and form one-dimensional channels along the *a*-axis. The BO_4 tetrahedra extend toward the channel to serve as one of the chromate chemisorption sites. Within the channels are found three chromate ions, which are chemically bonded to the aluminoborate layer. One chromate ion (CrA, 77% occupancy) is connected to an AlO_6 octahedron (Figure 5c), one (CrB, 32%) to both an AlO_6 octahedron and a BO_4 tetrahedron, and the third chromate ion (CrC, 24%) is connected to two AlO_6 octahedra, which are unusually formed during the ion-exchange process. The chromate ions are further stabilized via hydrogen bonding to the framework. There are in total 5.25 chromate ions per unit cell, which gives a formula of $H_{0.22}{\cdot}Al_2BO_{4.3}{\cdot}(HCrO_4)_{0.22}{\cdot}2.64H_2O$. The chromate ions CrB and CrC are too close to each other and cannot exist simultaneously. If these sites are fully occupied, they could accommodate eight chromate ions. There are other sites with similar local environments as the binding sites, CrA, CrB, and CrC, that may absorb additional chromate ions (Figure 5a). With the current cRED data, only three partially occupied chromate ion sites are found.

Effect of pH on Cr(VI) Adsorption

Hydrolytic stability is important for the long-term usage of ion exchangers in aqueous solution. Figure S8 shows the PXRD patterns of BAC(10) immersed in solutions with various pH values for 24 h under stirring, which indicates that BAC(10) has excellent hydrolytic stability in solutions with the pH range from 2 to 10.5. When the pH reaches 12, obvious dissolution of BAC(10) and formation of crystalline $Al(OH)_3$ (JCPDE card no. 20-0011) are observed. A further slight increase in pH (pH = 12.5) leads to the complete dissolution of BAC(10) and formation of highly crystalline $Al(OH)_3$. These results indicate that BAC(10) has excellent stability in acidic, neutral, and mildly basic solutions.

Figure 6 shows the influence of the initial pH of the solution on the removal efficiency of Cr(VI) and on the equilibrium pH. When the initial pH is increased from 2 to 10.5, the removal efficiency orderly decreases from 94.9 to 81.5% (initial concentration of Cr(VI): 50 mg/L and solid/liquid ratio: 2 g/L). Notably, the equilibrium pH maintains in the range of 3.77 to 5.02 even though the initial pH ranges from 2 to 10.5, demonstrating the excellent acidic/basic buffer ability of BAC(10). This might be due to the exchange-in of OH^- and exchange-out of Cl^-. When the initial pH rises to 12, a sharp decline in Cr(VI) removal efficiency to 17.2% and a dramatic increase in the equilibrium pH to 10.95 are observed. The optimal removal efficiency for Cr(VI) is 95.2% when the initial solution pH is 3.

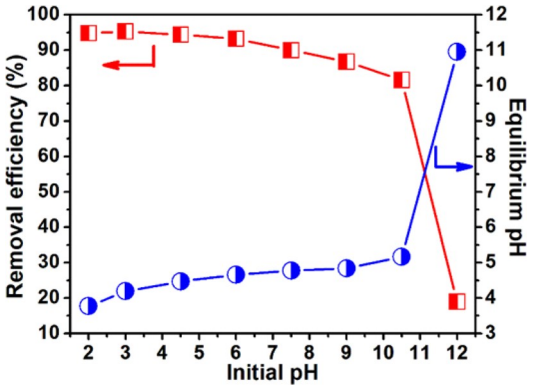

Figure 6. Influence of the initial pH on the removal efficiency (red line, left axis) and the corresponding equilibrium pH (blue line, right axis). The initial concentration of Cr(VI) is 50 mg/L and the solid/liquid ratio is 2 g/L.

In the solution containing Cr(VI), the predominant species of Cr(VI) is $HCrO_4^-$ when the pH is less than 6.5 and CrO_4^{2-} when the pH is greater than 6.5 (Figure S9).[53,54] For capturing one $HCrO_4^-$ anion, BAC(10) needs to release one Cl^-, while two Cl^- anions will be needed to capture one CrO_4^{2-}. Therefore, more CrO_4^{2-} content in solution will lead to a lower removal efficiency. In this study, when the initial pH is in the range of 2 to 10.5, the equilibrium pH is in the range of 3.77 to 5.02, at which the Cr(VI) species mainly exists in the form of $HCrO_4^-$ (Figure S9). With the increase of pH, the removal efficiency of Cr(VI) slightly decreases (Figure 6), which is due to the competitive adsorption of more OH^- on BAC(10). Further increasing the initial pH from 10.5 to 12 results in the dramatic increase of the equilibrium pH from about 5.02 to 10.95 (Figure 6) at which Cr(VI) exists mainly in the form of CrO_4^{2-} (Figure S9). In addition, the crystallinity of BAC(10) decreases significantly and $Al(OH)_3$ starts to be formed at such pH (Figure S8). Thus, a sudden drop in Cr(VI) removal efficiency is expected when the initial pH reaches 12. It has been reported that cationic framework materials, such as metal oxides,[55] cationic MOFs,[56] LDHs,[4] and AERs,[20] have shown strong dependence on the pH of solution for Cr(VI) removal and the optimal pH for Cr(VI) adsorption of these materials is usually 3 to 5. Unlike these materials, BAC(10) exhibits a wide working pH range from 2 to 10.5 and such a superior feature makes it promising in practical applications for Cr(VI) capture.

Adsorption Kinetics and Adsorption Isotherms of Cr(VI) on BAC(10)

The adsorption kinetics of Cr(VI) on BAC(10) is presented in Figure 7a (initial concentration of Cr(VI): 20 mg/L; solid/liquid ratio: 2 g/L; and initial pH: 3). Meanwhile, we selected the commercial AER (IRN78) and a calcined layered double hydroxide (CLDH) for comparison. As shown in Figure 7a, at the contact time of 10 min, the removal efficiency of BAC(10), IRN78, and CLDH is 66.9, 52.8, and 29.9%, respectively. When the contact time is extended to 60 min, the corresponding removal efficiency is increased to 97.4, 97.9, and 69.5%, respectively. On further extending the contact time, the removal efficiency of BAC(10) and IRN78 becomes almost constant, indicating that the adsorption equilibrium has been achieved at the contact time of 60 min. However, the adsorption equilibrium of CLDH can only be reached at the contact time of 150 min. The UV−vis spectra were acquired to monitor the concentration of Cr(VI) in solution as a function of the contact time of 0, 10, 20, 40, 60, and 90 min. As shown in Figure 7b, the intensity of the adsorption peak of $Cr_2O_7^{2-}$ at 352 nm in the UV−vis spectra of Cr(VI) in aqueous solution at various adsorption times quickly decreases within only 10 min and does not show further decrease after 60 min, suggesting that the anion-exchange process is completed. The inset photographs of Figure 7b also show that the solution changes to colorless within 60 min, indicating that BAC(10)

https://doi.org/10.1021/jacsau.2c00237
JACS Au 2022, 2, 1669−1678

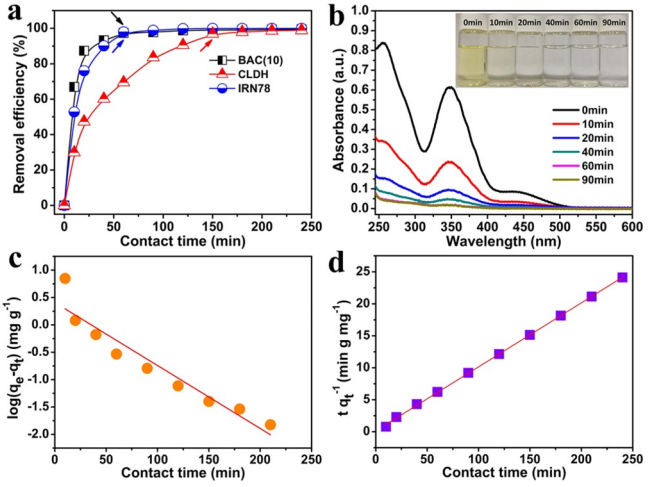

Figure 7. (a) Adsorption kinetics of Cr(VI) on BAC(10), IRN78, and CLDH. (b) UV−vis spectra of Cr(VI) in aqueous solution at various adsorption times by BAC(10). The inset shows the corresponding photographs. (c) Linear fitting with a pseudo-first-order kinetic model for BAC(10). (d) Linear fitting with a pseudo-second-order kinetic model for BAC(10).

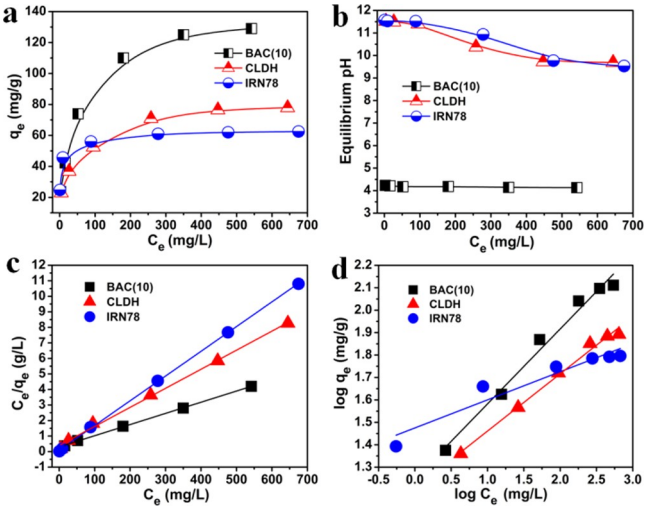

Figure 8. (a) Adsorption isotherms of Cr(VI) on BAC(10), IRN78, and CLDH; (b) the corresponding equilibrium pH; and (c) Langmuir linear plots and (d) Freundlich linear plots for adsorption isotherms of Cr(VI) on BAC(10), IRN78, and CLDH.

has a fast adsorption rate for Cr(VI), which is consistent with the adsorption kinetics results and UV−vis analysis. Compared to the cationic MOFs, BAC(10) also exhibits an advance in the removal rate. For example, more than 24 h are needed for ABT·2ClO_4[23] and 1-SO_4,[24] two MOFs with the fastest adsorption kinetics of Cr(VI), to reach the adsorption equilibrium. The fast adsorption kinetics of BAC(10) makes it highly suitable for practical applications.

The adsorption kinetics of BAC(10) is fitted by the linear pseudo-first-order equation and linear pseudo-second-order equation (eqs S1 and S2), respectively. The kinetic parameters and the correlation coefficients (R^2) are calculated on the basis of line regression (Figure 7c,d) and are listed in Table S2. The fitting plot with the pseudo-second-order model shows a better linearity (R^2 = 0.999) compared to the pseudo-first-order model (R^2 = 0.978), which confirms that the adsorption kinetics of BAC(10) follows the pseudo-second-order model, that is, a chemical adsorption process. The fitting plots in Figures S10, S11 and the data in Table S2 show that the adsorption kinetics of IRN78 (R^2 = 0.999) and CLDH (R^2 = 0.997) also follows the pseudo-second-order model, which is consistent with the results previously reported.[4,21]

The adsorption isotherms of Cr(VI) on BAC(10), CLDH, and IRN78 are illustrated in Figure 8a and the corresponding equilibrium pH values are plotted in Figure 8b (initial concentration of Cr(VI): 50−800 mg/L; solid/liquid ratio: 2 g/L; initial pH: 3; and contact time: 12 h under stirring). Both Langmuir and Freundlich models (eqs S3 and S4) are used to fit the experimental data and the results are presented in Figure 8c,d, respectively. The adsorption parameters and the correlation coefficients (R^2) on the basis of line regression (Figure 8c,d) are listed in Table S3. The fitting plots in Figure 8c,d and the data in Table S3 clearly show that the Langmuir model provides a better description of the adsorption behavior of Cr(VI) than the Freundlich model does, indicating a monolayer coverage of Cr(VI) anions on the internal surface of BAC(10), CLDH, and IRN-78. According to the Langmuir fitting, the maximum adsorption capacity (q_m) for Cr(VI) on BAC(10) is 139.1 mg/g, which is much higher than those on CLDH (81.43 mg/g) and IRN78 (62.77 mg/g), consistent with the previously reported values for CLDH and IRN78.[48,57] Table S4 summarizes the maximum adsorption capacities for Cr(VI) adsorption on typical anion exchangers such as cationic MOFs, LDHs, and AERs. Obviously, the maximum adsorption capacity of Cr(VI) on BAC(10) has outperformed most of them and is just less than that of MOFs of MOR-2.[58] The results in Figure 8b show that the equilibrium solutions containing BAC(10) are acidic (pH = 4−4.5), while those containing CLDH or IRN78 are basic (pH = 9.5−11.6) even though they have the same initial pH of 3.0. As discussed above, the distribution of Cr(VI) species is strongly affected by the solution pH. The Cr(VI) species mainly exists in the form of CrO_4^{2-} in the basic medium (pH > 6.5) and thus the adsorption capacity of the anion exchanger will be seriously inhibited. This is an important reason why BAC(10) has higher adsorption capacity for Cr(VI) than IRN78 and CLDH.

Adsorption Selectivity, Removal Efficiency, and Recyclability of BAC(10)

In addition to Cr(VI), polluted water usually contains other types of anions such as Cl^-, NO_3^-, HCO_3^-, and CO_3^{2-}. The existence of such anions apparently has a negative influence on the removal of Cr(VI) due to competitive adsorption. Hence, efficient removal of Cr(VI) from waste water is still a great challenge in the presence of large excess of competing anions. Here, we investigated the removal efficiency of BAC(10) on Cr(VI) in the presence of competitive anions of NO_3^-, Br^-, Cl^-, HCO_3^-, F^-, or CO_3^{2-} at various concentrations and the results are shown in Figure 9a. The initial concentration of Cr(VI) is 20.8 mg/L (0.4 mM), and the concentration of competitive anions is 0, 0.4, 2, 4, or 8 mM. The solid/liquid ratio is 2 g/L. To exclude the interference of pH, all the initial pH values are adjusted to 7. The results in Figure 9a show that the monovalent anions of NO_3^-, Br^-, Cl^-, and HCO_3^- have negligible influence on the removal efficiency of BAC(10) for Cr(VI) even under 20 times (8 mM) excess dose. The removal efficiency only decreases by 12.5% at the maximum even in the presence of 20 times excess of F^- (8 mM). Unlike monovalent anions, a large amount of CO_3^{2-} can adversely affect the adsorption of Cr(VI) and the removal efficiency decreased by

https://doi.org/10.1021/jacsau.2c00237
JACS Au 2022, 2, 1669−1678

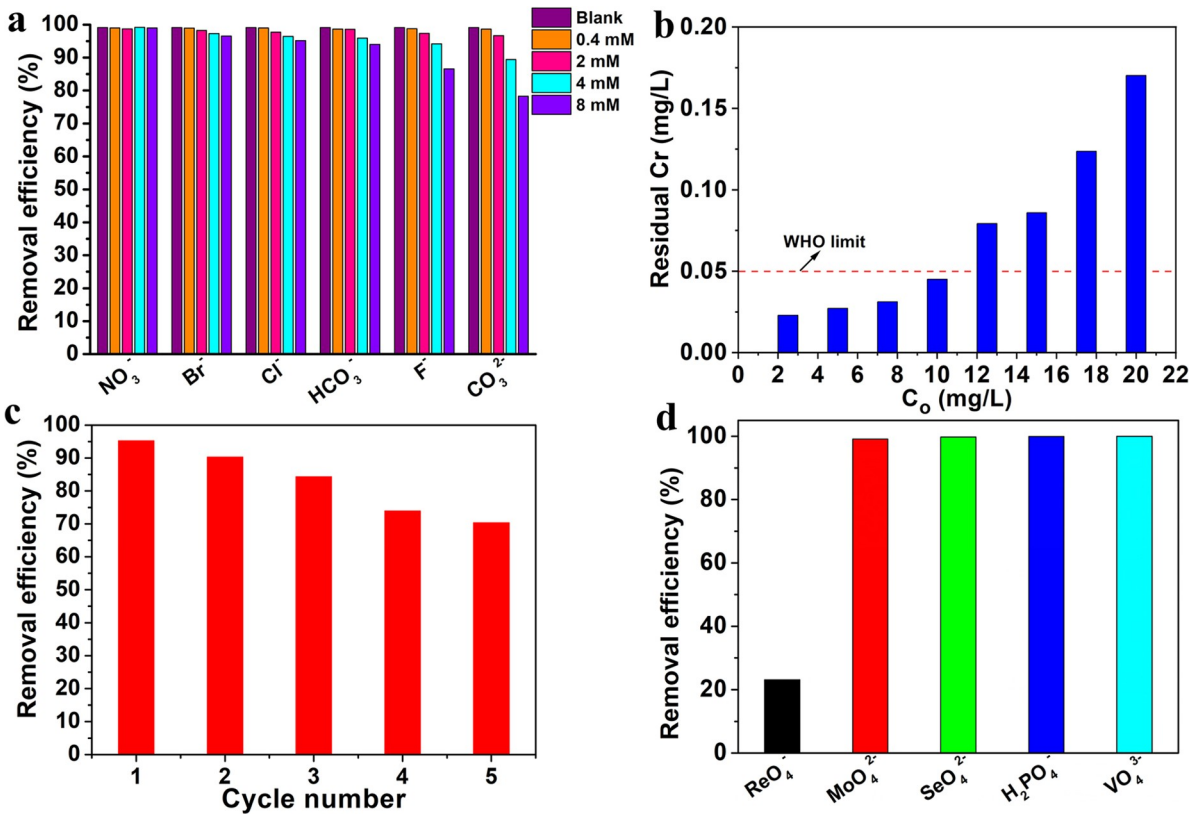

Figure 9. (a) Influence of competitive anions of NO_3^-, Br^-, Cl^-, HCO_3^-, F^-, and CO_3^{2-} on Cr(VI) removal by BAC(10); (b) removal efficiency of BAC(10) for Cr(VI) from aqueous solution prepared from DI water and tap water at low concentrations; (c) five cycles of adsorption−desorption of Cr(VI) on BAC(10); and (d) removal efficiency of ReO_4^-, MoO_4^{2-}, SeO_4^{2-}, $H_2PO_4^-$, and VO_4^{3-} by BAC(10).

20.8% in the presence of 8 mM CO_3^{2-} (20 times excess). Although the presence of large excess of CO_3^{2-} has a relative obviously negative influence on the removal efficiency of BAC(10) for Cr(VI), it is still obviously superior to many other anion exchangers, such as Ni/Mg/Al-LDHs[59] and UiO-66-NH_2@silica.[60] This may be ascribed to the excellent acidic/basic buffer ability of BAC(10) as described above. These results indicate that BAC(10) can selectively capture Cr(VI) even in the presence of large excess of competitive anions.

Although many adsorbents have excellent adsorption capacity for Cr(VI), it is difficult to reduce moderate and trace levels of Cr(VI) below the maximum allowable discharge standard defined by the WHO (0.05 mg/L).[6] Figure 9b presents the residual Cr(VI) concentration of the solution treated by BAC(10) with a solid/liquid ratio of 2 g/L. The initial concentration varied from 2.5 to 20 mg/L. The results show that the residual Cr(VI) concentration of the solution is lower than 0.05 mg/L after the treatment of BAC(10) if the initial concentration of Cr(VI) does not exceed 10 mg/L, which is below the allowed safe levels of WHO for drinking water as well as China and European Union. These results demonstrate that BAC(10) has excellent removal efficiency for low Cr(VI) concentration solutions, which makes it a promising material in practical applications for deep treatment of Cr(VI)-contaminated water. Combining the outstanding selectivity and depth removal performance of BAC(10) for Cr(VI) and the physicochemical and structural properties of Cr(VI)@BAC(10), we can conclude that the adsorption mechanism is based on the following: (i) ion exchange as the main mechanism of BAC(10) for Cr(VI) removal; (ii) formation of chemical bonds between the partial chromate ions and the inorganic sheet; and (iii) electrostatic interactions between the Cr(VI) anions and positively charged framework of BAC(10).

Furthermore, the recyclability of BAC(10) was investigated. The Cr(VI)@BAC(10) samples could be regenerated by a facile ion-exchange process method in a NaCl solution (detailed information is provided in the Supporting Information). Figure 9c shows the removal efficiency of BAC(10) for Cr(VI) in five cycles of adsorption−desorption process. After the first cycle, the removal efficiency decreases from 95.2 to 90.3%. Even at the fifth adsorption−desorption process, the removal efficiency of 70.3% can still be reached. The PXRD patterns of regenerated BAC(10) samples show that the structure is retained after multiple cycles (Figure S12). The decrease in removal efficiency with the increase in the number of cycles might be due to the strong affinity and the formation of chemical bonding between partial Cr(VI) and the framework of BAC(10), which leads to the incomplete replacement of Cr(VI) anions with Cl^- in the regeneration process. The EDS spectra and photographs of the regenerated BAC(10) samples further demonstrate the existence of undesorbed Cr(VI) in the regenerated BAC(10) (Figures S13, S14).

In addition to Cr(VI), many pollutants inherently exist in their oxyanion forms, such as ReO_4^-, MoO_4^{2-}, SeO_4^{2-}, $H_2PO_4^-$, and VO_4^{3-}. Among these oxyanions, ReO_4^- is employed as the surrogate of TcO_4^- (^{99}Tc), which is a highly problematic radioactive waste;[61] $H_2PO_4^-$ is one of the main causes for water eutrophication; MoO_4^{2-}, SeO_4^{2-}, and VO_4^{3-} are also harmful oxyanions to human health.[62−64] The removal efficiency of BAC(10) for ReO_4^-, MoO_4^{2-}, SeO_4^{2-}, $H_2PO_4^-$,

https://doi.org/10.1021/jacsau.2c00237
JACS Au 2022, 2, 1669−1678

and VO_4^{3-} is shown in Figure 9d. The initial concentrations of Re, Mo, Se, P, and V were 20 mg/L. The results show that the removal efficiency of BAC(10) for MoO_4^{2-}, SeO_4^{2-}, $H_2PO_4^-$, and VO_4^{3-} is over 99%, while for ReO_4^-, it is relatively low (29.1%). The results clearly show that BAC(10) also has excellent removal ability for MoO_4^{2-}, SeO_4^{2-}, $H_2PO_4^-$, and VO_4^{3-}.

CONCLUSIONS

Highly crystalline aluminoborate BAC(10) with a pure inorganic 2D cationic framework is hydrothermally synthesized with cost-effective source materials, and the structure of chromate ion-exchanged BAC(10) has been solved by cRED. The anion exchange property of BAC(10) for Cr(VI) from aqueous solution is superior to the commercial anion resin and LDHs with the maximum adsorption capacity and adsorption kinetics of Cr(VI). Owing to the acidic/basic buffer ability, BAC(10) exhibits a broad working pH range of 2−10.5 and excellent selectivity for Cr(VI) even in the presence of large amounts of excessive competitive anions. In addition, BAC(10) exhibits outstanding selectivity and depth removal performance for Cr(VI). The investigation on structural analysis and adsorption mechanism confirms that the removal of Cr(VI) from aqueous solution is achieved via the anion exchange of $HCrO_4^-$ with freely mobile Cl^- inside the structure of BAC(10) and formation of chemical bonds between the partial chromate ions and the inorganic sheet, which results in excellent selectivity for Cr(VI). The excellent performance and low cost make BAC(10) a promising material in wastewater treatment for Cr(VI) removal. BAC(10) also exhibits excellent removal efficiency for other harmful oxyanions such as MoO_4^{2-}, SeO_4^{2-}, $H_2PO_4^-$, and VO_4^{3-} from aqueous solution. To further investigate the possibility of use of BAC(10) in practical applications, we will conduct large-scale synthesis of BAC(10) and manufacture it into macroscopic structures such as granules, pellets, cylinders, or membranes to meet the requirement for practical applications.

ASSOCIATED CONTENT

Supporting Information

The Supporting Information is available free of charge at https://pubs.acs.org/doi/10.1021/jacsau.2c00237.

Full experimental procedures, cRED data, kinetic parameters, Langmuir and Freundlich isotherm parameters, XRD patterns, SEM and TEM images, N_2 adsorption−desorption isotherms, and EDS mapping profiles, and supporting tables (PDF)

AUTHOR INFORMATION

Corresponding Authors

Wenfu Yan − *State Key Laboratory of Inorganic Synthesis and Preparative Chemistry, College of Chemistry, Jilin University, Changchun 130012, P. R. China;* orcid.org/0000-0002-1000-6559; Email: yanw@jlu.edu.cn

Xiaodong Zou − *Department of Materials and Environmental Chemistry, Stockholm University, Stockholm SE-106 91, Sweden;* orcid.org/0000-0001-6748-6656; Email: xzou@mmk.su.se

Jihong Yu − *State Key Laboratory of Inorganic Synthesis and Preparative Chemistry, College of Chemistry, Jilin University, Changchun 130012, P. R. China; International Center of Future Science, Jilin University, Changchun 130012, P.R. China;* orcid.org/0000-0003-1615-5034; Email: jihong@jlu.edu.cn

Authors

Shuang Wang − *State Key Laboratory of Inorganic Synthesis and Preparative Chemistry, College of Chemistry, Jilin University, Changchun 130012, P. R. China; College of Chemistry and Chemical Engineering, Henan Province Function-Oriented Porous Materials Key Laboratory, Luoyang Normal University, Luoyang 471934, P.R. China;* orcid.org/0000-0003-4224-9122

Pu Bai − *State Key Laboratory of Inorganic Synthesis and Preparative Chemistry, College of Chemistry, Jilin University, Changchun 130012, P. R. China*

Magdalena Ola Cichocka − *Department of Materials and Environmental Chemistry, Stockholm University, Stockholm SE-106 91, Sweden;* Present Address: Institute for Metallic Materials, Leibniz Institute for Solid State and Materials Research Dresden, 01069 Dresden, Germany (M.O.C.)

Jung Cho − *Department of Materials and Environmental Chemistry, Stockholm University, Stockholm SE-106 91, Sweden*

Tom Willhammar − *Department of Materials and Environmental Chemistry, Stockholm University, Stockholm SE-106 91, Sweden;* orcid.org/0000-0001-6120-1218

Yunzheng Wang − *State Key Laboratory of Inorganic Synthesis and Preparative Chemistry, College of Chemistry, Jilin University, Changchun 130012, P. R. China*

Complete contact information is available at: https://pubs.acs.org/10.1021/jacsau.2c00237

Author Contributions

All authors have given approval to the final version of the manuscript. S.W., P.B., and M.O.C. contributed equally.

Notes

The authors declare no competing financial interest.

ACKNOWLEDGMENTS

We acknowledge the financial support from the National Key Research and Development Program of China (2021YFA1500401 and 2021YFA1501202), the National Natural Science Foundation of China (U1967215, 21835002, and 21621001), the 111 Project (B17020), the Key Science and Technology Program of Henan Province (212102210574), and the Swedish Research Council (VR, 2017-04321).

REFERENCES

(1) Mon, M.; Bruno, R.; Ferrando-Soria, J.; Armentano, D.; Pardo, E. Metal-Organic Framework Technologies for Water Remediation: Towards a Sustainable Ecosystem. *J. Mater. Chem. A* **2018**, *6*, 4912−4947.

(2) Keith, L. H.; Telliard, W. A. Priority Pollutants I: A Perspective View. *Environ. Sci. Technol.* **1979**, *13*, 416−423.

(3) Bailey, S.; Olin, T. J.; Bricka, R. M.; Adrian, D. D. A Review of Potentially Low-Cost Sorbents for Heavy Metals. *Water Res.* **1999**, *33*, 2469−2479.

(4) Li, Y.; Gao, B.; Wu, T.; Sun, D.; Li, X.; Wang, B.; Lu, F. Hexavalent Chromium Removal from Aqueous Solution by Adsorption on Aluminum Magnesium Mixed Hydroxide. *Water Res.* **2009**, *43*, 3067−3075.

(5) Jin, W.; Du, H.; Zheng, S.; Zhang, Y. Electrochemical Processes for the Environmental Remediation of Toxic Cr(VI): A Review. *Electrochim. Acta* **2016**, *191*, 1044−1055.
(6) World Health Organization, Guidelines for Drinking-Water Quality, 2004.
(7) Ministry of Health, Standardization Administration of the People's Republic of China, Standards for Drinking Water Quality (GB 5749-2006), 2006.
(8) G, D., *Directive 98/83/EC of 3 November 1998 on the Quality of Water Intended for Human Consumption*; Council of the European Union Brussels: Belgium, 1998; vol *330*, pp 32−54.
(9) Gheju, M.; Balcu, I. Removal of Chromium from Cr(VI) Polluted Wastewaters by Reduction with Scrap Iron and Subsequent Precipitation of Resulted Cations. *J. Hazard. Mater.* **2011**, *196*, 131−138.
(10) Acharya, R.; Lenka, A.; Parida, K. Magnetite Modified Amino Group Based Polymer Nanocomposites Towards Efficient Adsorptive Detoxification of Aqueous Cr(VI): A Review. *J. Mol. Liq.* **2021**, *337*, No. 116487.
(11) Wang, J. W.; Qiu, F. G.; Wang, P.; Ge, C. J.; Wang, C. C. Boosted Bisphenol A and Cr(VI) Cleanup over Z-Scheme WO_3/MIL-100(Fe) Composites under Visible Light. *J. Cleaner Prod.* **2021**, *279*, No. 123408.
(12) Roy Choudhury, P.; Majumdar, S.; Sahoo, G. C.; Saha, S.; Mondal, P. High Pressure Ultrafiltration CuO/Hydroxyethyl Cellulose Composite Ceramic Membrane for Separation of Cr(VI) and Pb(II) from Contaminated Water. *Chem. Eng. J.* **2018**, *336*, 570−578.
(13) Li, Z. J.; Zhang, Q.; Xue, H. D.; Zheng, X. D.; Qi, H. L.; Li, H. C. A Versatile Cationic Organic Network Adsorbent for the Highly Efficient Removal of Diverse Water Contaminants. *Adv. Mater. Interfaces* **2021**, *8*, No. 2100016.
(14) Zhao, X. L.; Yu, X. Z.; Wang, X. Y.; Lai, S. J.; Sun, Y. Y.; Yang, D. J. Recent Advances in Metal-Organic Frameworks for the Removal of Heavy Metal Oxoanions from Water. *Chem. Eng. J.* **2021**, *407*, No. 127221.
(15) Fei, H.; Han, C. S.; Robins, J. C.; Oliver, S. R. J. A Cationic Metal-Organic Solid Solution Based on Co(II) and Zn(II) for Chromate Trapping. *Chem. Mater.* **2013**, *25*, 647−652.
(16) Dragan, E. S.; Humelnicu, D. Contribution of Cross-Linker and Silica Morphology on Cr(VI) Sorption Performances of Organic Anion Exchangers Embedded into Silica Pores. *Molecules* **2020**, *25*, 1249.
(17) Bekchanov, D.; Mukhamediev, M.; Lieberzeit, P.; Babojonova, G.; Botirov, S. Polyvinylchloride-Based Anion Exchanger for Efficient Removal of Chromium (VI) from Aqueous Solutions. *Polym. Adv. Technol.* **2021**, *32*, 3995−4004.
(18) Li, J.; Wang, X.; Zhao, G.; Chen, C.; Chai, Z.; Alsaedi, A.; Hayat, T.; Wang, X. Metal-Organic Framework-Based Materials: Superior Adsorbents for the Capture of Toxic and Radioactive Metal Ions. *Chem. Soc. Rev.* **2018**, *47*, 2322−2356.
(19) Li, Y.; Yang, Z.; Wang, Y.; Bai, Z.; Zheng, T.; Dai, X.; Liu, S.; Gui, D.; Liu, W.; Chen, M.; Chen, L.; Diwu, J.; Zhu, L.; Zhou, R.; Chai, Z.; Albrecht-Schmitt, T. E.; Wang, S. A Mesoporous Cationic Thorium-Organic Framework that Rapidly Traps Anionic Persistent Organic Pollutants. *Nat. Commun.* **2017**, *8*, 1354.
(20) Atia, A. A. Synthesis of a Quaternary Amine Anion Exchange Resin and Study of its Adsorption Behaviour for Chromate Oxyanions. *J. Hazard. Mater.* **2006**, *137*, 1049−1055.
(21) Edebali, S.; Pehlivan, E. Evaluation of Amberlite IRA96 and Dowex 1×8 Ion-Exchange Resins for the Removal of Cr(VI) from Aqueous Solution. *Chem. Eng. J.* **2010**, *161*, 161−166.
(22) Zou, Y.-H.; Liang, J.; He, C.; Huang, Y.-B.; Cao, R. A Mesoporous Cationic Metal-Organic Framework with a High Density of Positive Charge for Enhanced Removal of Dichromate from Water. *Dalton Trans.* **2019**, *48*, 6680−6684.
(23) Desai, A. V.; Manna, B.; Karmakar, A.; Sahu, A.; Ghosh, S. K. A Water-Stable Cationic Metal-Organic Framework as a Dual Adsorbent of Oxoanion Pollutants. *Angew. Chem., Int. Ed.* **2016**, *55*, 7811−7815.
(24) Sheng, D.; Zhu, L.; Xu, C.; Xiao, C.; Wang, Y.; Wang, Y.; Chen, L.; Diwu, J.; Chen, J.; Chai, Z.; Albrecht-Schmitt, T. E.; Wang, S. Efficient and Selective Uptake of TcO_4^- by a Cationic Metal-Organic Framework Material with Open Ag^+ Sites. *Environ. Sci. Technol.* **2017**, *51*, 3471−3479.
(25) Zhu, L.; Sheng, D.; Xu, C.; Dai, X.; Silver, M. A.; Li, J.; Li, P.; Wang, Y.; Wang, Y.; Chen, L.; Xiao, C.; Chen, J.; Zhou, R.; Zhang, C.; Farha, O. K.; Chai, Z.; Albrecht-Schmitt, T. E.; Wang, S. Identifying the Recognition Site for Selective Trapping of $^{99}TcO_4^-$ in a Hydrolytically Stable and Radiation Resistant Cationic Metal-Organic Framework. *J. Am. Chem. Soc.* **2017**, *139*, 14873−14876.
(26) Sharma, S.; Let, S.; Desai, A. V.; Dutta, S.; Karuppasamy, G.; Shirolkar, M. M.; Babarao, R.; Ghosh, S. K. Rapid, Selective Capture of Toxic Oxo-Anions of Se(IV), Se(VI) and As(V) from Water by an Ionic Metal-Organic Framework (iMOF). *J. Mater. Chem. A* **2021**, *9*, 6499−6507.
(27) Zou, Y.-H.; Huang, Y.-B.; Si, D.-H.; Yin, Q.; Wu, Q.-J.; Weng, Z.; Cao, R. Porous Metal-Organic Framework Liquids for Enhanced CO_2 Adsorption and Catalytic Conversion. *Angew. Chem., Int. Ed.* **2021**, *60*, 20915−20920.
(28) Liang, J.; Chen, R.-P.; Wang, X.-Y.; Liu, T.-T.; Wang, X.-S.; Huang, Y.-B.; Cao, R. Postsynthetic Ionization of an Imidazole-Containing Metal-Organic Framework for the Cycloaddition of Carbon Dioxide and Epoxides. *Chem. Sci.* **2017**, *8*, 1570−1575.
(29) Wang, Y.; Wang, S.; Li, X.; Bai, P.; Yan, W.; Yu, J. Layered Inorganic Cationic Frameworks Beyond Layered Double Hydroxides (LDHs): Structures and Applications. *Eur. J. Inorg. Chem.* **2020**, 4055−4063, DOI: 10.1002/ejic.202000710.
(30) Fang, Q. Z.; Ye, S. J.; Yang, H. L.; Yang, K. H.; Zhou, J. W.; Gao, Y.; Lin, Q. Y.; Tan, X. F.; Yang, Z. Z. Application of Layered Double Hydroxide-Biochar Composites in Wastewater Treatment: Recent Trends, Modification Strategies, and Outlook. *J. Hazard. Mater.* **2021**, *420*, No. 126569.
(31) Chubar, N.; Gilmour, R.; Gerda, V.; Micusik, M.; Omastova, M.; Heister, K.; Man, P.; Fraissard, J.; Zaitsev, V. Layered Double Hydroxides as the Next Generation Inorganic Anion Exchangers: Synthetic Methods Versus Applicability. *Adv. Colloid Interface Sci.* **2017**, *245*, 62−80.
(32) Sajid, M.; Jillani, S. M. S.; Baig, N.; Alhooshani, K. Layered Double Hydroxide-Modified Membranes for Water Treatment: Recent Advances and Prospects. *Chemosphere* **2022**, *287*, No. 132140.
(33) Huang, S. Q.; Ouyang, T.; Chen, J. Y.; Wang, Z.; Liao, S. Q.; Li, X. Y.; Liu, Z. Q. Synthesis of Nickel-Iron Layered Double Hydroxide via Topochemical Approach: Enhanced Surface Charge Density for Rapid Hexavalent Chromium Removal. *J. Colloid Interface Sci.* **2022**, *605*, 602−612.
(34) Zhang, Y. Z.; Qin, J. F.; Wang, X. J.; Chen, Z. G.; Zheng, X. W.; Chen, Y. X. Advanced Treatment of Phosphorus-Containing Tail Water by Fe-Mg-Zr Layered Double Hydroxide Beads: Performance and Mechanism. *J. Environ. Manage.* **2021**, *296*, No. 113203.
(35) Jung, K. W.; Lee, S. Y.; Choi, J. W.; Hwang, M. J.; Shim, W. G. Synthesis of Mg-Al Layered Double Hydroxides-Functionalized Hydrochar Composite Via an in Situ One-Pot Hydrothermal Method for Arsenate and Phosphate Removal: Structural Characterization and Adsorption Performance. *Chem. Eng. J.* **2021**, *420*, No. 129775.
(36) Tian, Q. Z.; Guo, B. L.; Sasaki, K. Influence of Silicate on the Structural Memory Effect of Layered Double Hydroxides for the Immobilization of Selenium. *J. Hazard. Mater.* **2020**, *395*, No. 122674.
(37) Qiu, X.; Sasaki, K.; Osseo-Asare, K.; Hirajima, T.; Ideta, K.; Miyawaki, J. Sorption of H_3BO_3/$B(OH)_4^-$ on Calcined Ldhs Including Different Divalent Metals. *J. Hazard. Mater.* **2015**, *445*, 183−194.
(38) Parker, L. M.; Milestone, N. B.; Newman, R. H. The Use of Hydrotalcite as an Anion Absorbent. *Ind. Eng. Chem. Res.* **1995**, *34*, 1196−1202.
(39) Fei, H.; Oliver, S. R. J. Copper Hydroxide Ethanedisulfonate: A Cationic Inorganic Layered Material for High-Capacity Anion Exchange. *Angew. Chem., Int. Ed.* **2011**, *50*, 9066−9070.

(40) Sergo, K. M.; Han, C. S.; Bresler, M. R.; Citrak, S. C.; Abdollahian, Y.; Fei, H.; Oliver, S. R. Erbium Hydroxide Ethanedisulfonate: A Cationic Layered Material with Organic Anion Exchange Capability. *Inorg. Chem.* **2015**, *54*, 3883−3888.
(41) Fei, H.; Pham, C. H.; Oliver, S. R. Anion Exchange of the Cationic Layered Material $[Pb_2F_2]^{2+}$. *J. Am. Chem. Soc.* **2012**, *134*, 10729−10732.
(42) Yang, H.; Fei, H. Exfoliation of a Two-Dimensional Cationic Inorganic Network as a New Paradigm for High-Capacity Cr(VI)-Anion Capture. *Chem. Commun.* **2017**, *53*, 7064−7067.
(43) Geng, F.; Matsushita, Y.; Mat, R.; Xin, H.; Tanaka, M.; Izumi, F.; Iyi, N.; Sasaki, T. General Synthesis and Structural Evolution of a Layered Family of $Ln_8(OH)_{20}Cl_4{\cdot}nH_2O$ (Ln = Nd, Sm, Eu, Gd, Tb, Dy, Ho, Er, Tm, and Y). *J. Am. Chem. Soc.* **2008**, *130*, 16344−16350.
(44) Zhu, L.; Zhang, L.; Li, J.; Zhang, D.; Chen, L.; Sheng, D.; Yang, S.; Xiao, C.; Wang, J.; Chai, Z.; Albrecht-Schmitt, T. E.; Wang, S. Selenium Sequestration in a Cationic Layered Rare Earth Hydroxide: A Combined Batch Experiments and Exafs Investigation. *Environ. Sci. Technol.* **2017**, *51*, 8606−8615.
(45) Wang, S.; Alekseev, E. V.; Diwu, J.; Casey, W. H.; Phillips, B. L.; Depmeier, W.; Albrecht-Schmitt, T. E. NDTB-1: A Supertetrahedral Cationic Framework That Removes TcO_4^- from Solution. *Angew. Chem., Int. Ed.* **2010**, *49*, 1057−1060.
(46) Yu, P.; Wang, S.; Alekseev, E. V.; Depmeier, W.; Hobbs, D. T.; Albrecht-Schmitt, T. E.; Phillips, B. L.; Casey, W. H. Technetium-99 MAS NMR Spectroscopy of a Cationic Framework Material that Traps TcO_4^- Ions. *Angew. Chem., Int. Ed.* **2010**, *49*, 5975−5977.
(47) Wang, S.; Yu, P.; Purse, B. A.; Orta, M. J.; Diwu, J.; Casey, W. H.; Phillips, B. L.; Alekseev, E. V.; Depmeier, W.; Hobbs, D. T.; Albrecht-Schmitt, T. E. Selectivity, Kinetics, and Efficiency of Reversible Anion Exchange with TcO_4^- in a Supertetrahedral Cationic Framework. *Adv. Funct. Mater.* **2012**, *22*, 2241−2250.
(48) Bai, P.; Dong, Z.; Wang, S.; Wang, X.; Li, Y.; Wang, Y.; Ma, Y.; Yan, W.; Zou, X.; Yu, J. A Layered Cationic Aluminum Oxyhydroxide as a Highly Efficient and Selective Trap for Heavy Metal Oxyanions. *Angew. Chem., Int. Ed.* **2020**, *59*, 19539−19544.
(49) Yu, J.; Xu, R.; Chen, J.; Yue, Y. On the Crystallisation and Nature of the Microporous Boron-Aluminium Oxo Chloride BAC(10). *J. Mater. Chem.* **1996**, *6*, 465−468.
(50) Hoffmann, M. M.; Darab, J. G.; Fulton, J. L. An Infrared and X-Ray Absorption Study of the Equilibria and Structures of Chromate, Bichromate, and Dichromate in Ambient Aqueous Solutions. *J. Phys. Chem. A* **2001**, *105*, 1772−1782.
(51) Desimoni, E.; Malitesta, C.; Zambonin, P.; Riviere, J. An X-Ray Photoelectron Spectroscopic Study of Some Chromium-Oxygen Systems. *Surf. Interface Anal.* **1988**, *13*, 173−179.
(52) Wan, W.; Sun, J.; Su, J.; Hovmoller, S.; Zou, X. Three-Dimensional Rotation Electron Diffraction: Software Red for Automated Data Collection and Data Processing. *J. Appl. Crystallogr.* **2013**, *46*, 1863−1873.
(53) Sengupta, A. K.; Clifford, D. Chromate Ion Exchange Mechanism for Cooling Water. *Ind. Eng. Chem. Fundam.* **1986**, *25*, 249−258.
(54) Mohan, D.; Pittman, C. U. J. Activated Carbons and Low Cost Adsorbents for Remediation of Tri- and Hexavalent Chromium from Water. *J. Hazard. Mater.* **2006**, *137*, 762−811.
(55) Rodrigues, L. A.; Maschio, L. J.; da Silva, R. E.; da Silva, M. L. Adsorption of Cr(VI) from Aqueous Solution by Hydrous Zirconium Oxide. *J. Hazard. Mater.* **2010**, *173*, 630−636.
(56) Li, L.-L.; Feng, X.-Q.; Han, R.-P.; Zang, S.-Q.; Yang, G. Cr(VI) Removal via Anion Exchange on a Silver-Triazolate MOF. *J. Hazard. Mater.* **2017**, *321*, 622−628.
(57) Xiao, L.; Ma, W.; Han, M.; Cheng, Z. The Influence of Ferric Iron in Calcined Nano-Mg/Al Hydrotalcite on Adsorption of Cr (VI) from Aqueous Solution. *J. Hazard. Mater.* **2011**, *186*, 690−698.
(58) Rapti, S.; Sarma, D.; Diamantis, S. A.; Skliri, E.; Armatas, G. S.; Tsipis, A. C.; Hassan, Y. S.; Alkordi, M.; Malliakas, C. D.; Kanatzidis, M. G.; Lazarides, T.; Plakatouras, J. C.; Manos, M. J. All in One Porous Material: Exceptional Sorption and Selective Sensing of Hexavalent Chromium by Using a Zr^{4+} MOF. *J. Mater. Chem. A* **2017**, *5*, 14707−14719.
(59) Lei, C.; Zhu, X.; Zhu, B.; Jiang, C.; Le, Y.; Yu, J. Superb Adsorption Capacity of Hierarchical Calcined Ni/Mg/Al Layered Double Hydroxides for Congo Red and Cr(VI) Ions. *J. Hazard. Mater.* **2017**, *321*, 801−811.
(60) El-Mehalmey, W. A.; Ibrahim, A. H.; Abugable, A. A.; Hassan, M. H.; Haikal, R. R.; Karakalos, S. G.; Zaki, O.; Alkordi, M. H. Metal-Organic Framework@Silica as a Stationary Phase Sorbent for Rapid and Cost-Effective Removal of Hexavalent Chromium. *J. Mater. Chem. A* **2018**, *6*, 2742−2751.
(61) Banerjee, D.; Kim, D.; Schweiger, M. J.; Kruger, A. A.; Thallapally, P. K. Removal of TcO_4^- Ions from Solution: Materials and Future Outlook. *Chem. Soc. Rev.* **2016**, *45*, 2724−2739.
(62) Afkhami, A.; Madrakian, T.; Amini, A. Mo(VI) and W(VI) Removal from Water Samples by Acid-Treated High Area Carbon Cloth. *Desalination* **2009**, *243*, 258−264.
(63) Cai, H.; Bao, H.; Zhang, X.; Lei, L.; Xiao, C. Highly Efficient Sorption of Selenate and Selenite onto a Cationic Layered Single Hydroxide via Anion Exchange and Inner-Sphere Complexation. *Chem. Eng. J.* **2021**, *420*, No. 129726.
(64) Song, H.-L.; Jiao, F.-P.; Jiang, X.-Y.; Yu, J.-G.; Chen, X.-Q.; Du, S.-L. Removal of Vanadate Anion by Calcined Mg/Al-CO_3 Layered Double Hydroxide in Aqueous Solution. *Trans. Nonferrous Met. Soc. China* **2013**, *23*, 3337−3345.

https://doi.org/10.1021/jacsau.2c00237
JACS Au 2022, 2, 1669−1678